1   **Original Article**

2   *Title:* **Looks do matter! Aortic arch shape following hypoplastic left heart**

3   **syndrome palliation correlates with cavopulmonary outcomes**

4   *Running Head:* **Aortic arch shape analysis in HLHS**

5   *Authors:* Jan L Bruse, MSc[1], Elena Cervi, MD[1], Kristin McLeod, PhD[2,3], Giovanni Biglino,

6   PhD[1], Maxime Sermesant, PhD[3], Xavier Pennec, PhD[3], Andrew M Taylor, MD[1], Silvia

7   Schievano, PhD[1], and Tain-Yen Hsia, MD[1*]; for the Modeling of Congenital Hearts Alliance

8   (MOCHA) Collaborative Group[4]

9   *Institutions and Affiliations*:

10   [1]Centre for Cardiovascular Imaging, University College London, Institute of Cardiovascular

11   Science & Cardiorespiratory Unit, Great Ormond Street Hospital for Children, London, UK

12   [2]Simula Research Laboratory, Cardiac Modeling Department, Oslo, Norway

13   [3]Inria, Asclepios Team, Sophia Antipolis, France

14   [4]MOCHA Collaborative Group: Andrew Taylor, Sachin Khambadkone, Silvia Schievano,
15   Marc de Leval, T. -Y. Hsia (University College London, UK); Edward Bove, Adam Dorfman
16   (University of Michigan, USA); G. Hamilton Baker, Anthony Hlavacek (Medical University
17   of South Carolina, USA); Francesco Migliavacca, Giancarlo Pennati, Gabriele Dubini
18   (Politecnico di Milano, Italy); Alison Marsden (University of California, USA); Irene
19   Vignon-Clementel (INRIA, France); Richard Figliola (Clemson University, USA).
20

24   ***Word Count:* 4447**

25   *Corresponding author:

26   T-Y Hsia, MD
27   Cardiac Unit
28   Great Ormond Street Hospital for Children, NHS Trust
29   London, WC1N 3JH, UK
30   Telephone: +44-(0)207-813-8159
31   Email: hsiat@gosh.nhs.uk

1 **Abstract**

2 Background: Aortic arch reconstruction following hypoplastic left heart syndrome (HLHS)

3 palliation can vary widely in shape and dimensions between patients. Arch morphology alone

4 may impact on cardiac function and outcome. We sought to uncover the relationship of arch

5 3D shape features with functional and short-term outcome data following total

6 cavopulmonary connection (TCPC).

7 Methods: Aortic arch shape models of 37 patients with HLHS (age 2.89±0.99 years) were

8 reconstructed from magnetic resonance data prior to TCPC completion. A novel, validated

9 statistical shape analysis method computed a 3D anatomic mean shape from the cohort, and

10 calculated the deformation vectors of the mean shape towards each patient's specific

11 anatomy. From these deformations, 3D shape features most related to ventricular ejection

12 fraction (EF), indexed end-diastolic volume (iEDV) and superior cavopulmonary pressure

13 (SCP) were extracted via partial least square regression analysis. Moreover, shape patterns

14 relating to length of ICU stay (LICU) and hospital stay (LOHS) following TCPC were

15 assessed.

16 Results: Distinct deformation patterns, which result in acutely mismatched aortic root and

17 ascending aorta, and gothic-like transverse arch, correlated with increased iEDV and higher

18 SCP, but not with EF. Moreover, specific arch morphology with pronounced transverse arch

19 and descending aorta mismatch correlated with longer LICU and LOHS following TCPC

20 completion.

21 Conclusion: Independent of hemodynamically important arch obstruction, altered aortic

22 morphology in HLHS patients appears to have important associations with higher SCP and

23 with short-term outcomes following TCPC completion as highlighted by statistical shape

24 analysis, which could act as adjunct to risk assessment in HLHS.

25 *Abstract Word Count:* **247**

Introduction

1
2

3 Stage 1 palliation for hypoplastic left heart syndrome (HLHS) requires a modified Damus-

4 Kay-Stansel procedure with reconstructive augmentation of the aortic arch, typically using a

5 homograft patch of varying sizes and shapes. As a consequence, the resultant morphology of

6 the neo-ascending aorta and aortic arch can be highly variable from patient to patient, in

7 addition to differing incidences of residual arch obstruction, dilatation, and tortuosity.

8 Recently, late systemic hypertension in patients following successful aortic coarctation repair

9 was found to relate to deranged aortic arch shape. (1) While in HLHS patients, residual

10 coarctation and recurrent arch obstruction are known to be associated with worse cardiac

11 function and poorer outcomes (2, 3), a recent study using wave intensity analysis has

12 demonstrated that aortic arch shape features such as grossly mismatched dimensions between

13 the transverse and descending aorta can also lead to maladaptive ventriculo-arterial coupling

14 and reduced ventricular ejection fraction. (4)

15 In this study, we sought to analyze in greater depth and detail arch shape features in patients

16 who have undergone Stage 1 Norwood aortic arch reconstruction. Being widely variable in

17 both shape and size, surgically reconstructed aortic arches in HLHS cannot be adequately

18 analyzed by traditional morphometric methods using only two-dimensional (2D) measures

19 such as lengths and diameters, since these are insufficient to provide a comprehensive

20 description of the multitude of morphological permutations. Therefore, we applied a novel,

21 validated three-dimensional (3D) statistical shape analysis method (SSM) that quantitatively

22 evaluates the ascending aorta/arch morphology as a single, contiguous 3D unit, without the

23 need for manually measuring the numerous dimensions. (5-7) We hypothesized that 3D arch

24 shape features extracted via the SSM are associated with the functional status of the Stage 2

25 superior cavopulmonary circulation, and with short-term clinical outcome following Stage 3

26 total cavopulmonary connection (TCPC).

Patients and Methods

Patient population

We retrospectively analyzed cardiovascular magnetic resonance (CMR) data of 37 patients (mean age 2.89 ± 0.99 years; 11 female) with HLHS as primary diagnosis who previously underwent Stage 1 Norwood-type aortic arch reconstruction (12 right ventricular to pulmonary arterial shunts, rest modified Blalock-Taussig shunts) and Stage 2 superior cavopulmonary (bi-directional Glenn) palliation. In all patients, the aortic arch reconstruction was performed with standard Daymus-Kay-Stansel followed by patch augmentation of the aortic arch using pulmonary arterial homograft, without coarctectomy. The homograft were fashioned per surgeon preference and expertise, but typically beginning with a triangular shaped patch. Nine patients had had either balloon dilatation due to aortic re-coarctation before, or concomitant aortic arch repair during, the Stage 2 procedure. In all patients, CMR examination had been carried out routinely in preparation for Stage 3 TCPC completion. Moreover, at the time of CMR and TCPC completion, none of the 37 patients had hemodynamically significant residual aortic arch obstruction requiring revision as determined by Doppler echocardiographic interrogation, done as part of the routine preTCPC assessment. Ethical approval was obtained for the use of image data for research purposes, and all parents/legal guardians gave informed consent for research use of the data.

CMR imaging and processing

CMR data were acquired during mid-diastolic rest using a 3D balanced, steady-state free precession (bSSFP) whole-heart sequence (1.5T Avanto MR scanner, Siemens Medical Solutions, Germany). 3D aortic arch volumes were segmented and processed manually using commercial software (Mimics, Materialise, Belgium) and exported as computational surface

meshes (Fig. 1b). The 3D arch models were cut consistently at the sub-annular plane and at the level of the diaphragm using The Vascular Modeling Toolkit (VMTK, (8)). Head and neck vessels, coronary arteries and the hypoplastic native aorta were removed as closely as possible to the neo-aortic arch to focus the examination to the ascending aorta/arch/descending aorta unit (Fig. 1a). Further, arch models were pre-aligned using an Iterative Closest Point algorithm (9) in VMTK. The cut and aligned 3D surface meshes of all 37 arches constituted the input for the SSM (Fig. 1c).

Clinical parameters

Ejection fraction (EF) and indexed end-diastolic volume (iEDV) based on combined blood volumes of the single right ventricle and the hypoplastic left ventricle were derived from CMR as functional parameters prior to TCPC completion. Moreover, the superior cavopulmonary pressures (SCP) of the Glenn connection, measured during CMR acquisition, were obtained in 33 patients (SCP was not measured in 4 patients). To assess short-term outcome following TCPC completion, length of stay in the intensive care unit (LICU) and the length of hospital stay (LOHS) post-TCPC completion were retrieved from clinical reports for all 37 patients.

Traditional morphometrics

The following traditional 2D and 3D morphometric parameters were measured manually from each aortic arch model in order to validate the SSM results: surface area (A_{surf}), volume (V), centerline length (CL_{length}), and centerline tortuosity (CL_{tort}) of the 3D arch models (10); area at the sub-annular plane (A_{ventr}); cross-sectional area of the native aorta at the site of anastomosis ($A_{nativeAo}$); and cross-sectional areas of the transverse arch (A_{trans}), at the isthmus (A_{isth}) and at the level of the diaphragm (A_{dia}) were measured manually as previously

1 described. (Fig. 2a) (4); aortic arch diameter at the level of the cavopulmonary connection

2 (T); and diameters of the ascending (D_{asc}) and of the descending aorta (D_{desc}) at the same

3 level, were measured from the 2D CMR whole-heart data. (Fig. 2b) Various ratios to reflect

4 changes in caliber/dimension were computed and all parameters were indexed with the

5 patient body surface area (BSA), when appropriate. (Table 1) Indexed parameters are marked

6 with a preceding lower case i.

7 **Statistical shape analysis method (SSM)**

8

9 From the 37 computational 3D surface meshes derived from the CMR data, the SSM

10 computes a single *template* (or *atlas*; i.e. the 3D anatomical mean shape). (Fig. 3a) From this

11 template or "prototype", a *forward approach* method then quantitatively re-creates each

12 patient's aortic arch shape by *deforming* the template aorta using a unique, patient-specific set

13 of deformation vectors. (11) This mean aorta can be transformed into the unique arch shape

14 of *each* of the 37 patients by applying the correct set of patient-specific deformations. Rather

15 than describing 3D shape as a collection of coordinates, points, or landmarks, each patient's

16 aorta shape is thus characterized by its unique set of deformation vectors. By gathering the 37

17 deformation vectors into one deformation matrix that contains all the 3D shape information

18 of the cohort, statistical analysis can be performed to assess how shape variability relates to

19 clinical parameters. (Fig. 3b)

20 Standard dimensionality reduction techniques such as principal component analysis (PCA)

21 can be applied to detect key contributors to 3D shape variability. (12) In this study we applied

22 *partial least squares regression* (PLS, a combination of PCA and linear regression) to the

23 deformation matrix, in order to extract 3D shape features (i.e. shape deformations) *most*

24 *correlated* to the clinical parameters. (12-13) Each extracted shape feature can be quantified

25 as deformations of, or deviation from, the template, denoted as low (-2 standard deviations,

1 SD) to high (+2SD). Furthermore, a *shape vector* is obtained to quantify the severity of the

2 extracted shape features within each of the 37 patients. (13) The patient-specific shape vector

3 can thus be seen as a numerical representation of each patient's collection of 3D shape

4 features, as a relation of deformation from the template.

5 For example, if a large cohort of mixed arch shapes with known pressure gradient were

6 analyzed in order to find an association between arch shape and pressure drop across the arch,

7 the SSM would create and then deform the mean template shape from an unobstructed aortic

8 arch with low pressure drop *towards* an obstructed arch with high pressure drops. In doing

9 this, the correlation between the derived shape vector and the measured pressure gradient

10 would reveal that most patients with arch narrowing had high pressure drops.

11 The analysis was carried out using the *Exoshape* code framework[1] to compute template and

12 deformation matrix and to extract 3D shape features related to the 5 clinical parameters via

13 PLS regression. (13) The SSM template shape was validated against the traditional

14 morphometric parameters. Prior to extracting shape features, size effects due to differences in

15 BSA between patients were removed as described previously. (5)

16 **Statistics**

17

18 Associations between morphometric parameters, shape vectors and clinical outcome

19 parameters were assessed via standard bi-variate correlation analyses. *Pearson's r* was

20 reported for parametric, normally distributed data, whereas *Kendall's τ* was reported for non-

21 parametric data. Non-normality was assumed if the Shapiro-Wilk test was significant;

22 significance was assumed at level $p<0.05$. Outliers in the data – subjects with the respective

23 analyzed clinical parameter and/or BSA more than ± 2 SD away from the population mean –

24 which may skew the results, were excluded from the PLS regression analysis known to be

---

[1]*http://www-sop.inria.fr/asclepios/projects/Health-e-Child/ShapeAnalysis/*

1 highly sensitive to these (14). All statistical tests were performed in SPSS (IBM SPSS

2 Statistics, SPSS Inc., USA).

Results

Template aorta

The template aorta, derived as the mean 3D aorta shape computed from the 37-patient cohort, had a fairly rounded overall arch shape with no distinct narrowing, but a slightly 'oversized' aortic root, ascending aorta and transverse arch that was significantly larger than the descending aorta (Fig. 4). The top view revealed marked tortuosity as well as irregular surface above the root. These features are typical following a Norwood-type aortic arch reconstruction. Table 2 demonstrates that the traditional morphometric parameters (such as the centerline length, volume and arch surface area) from the template were minimally different from the averaged measurement values from the 37 models, with an overall deviation of 2.17%, thus validating the representative average shape.

Correlation between shape features and clinical parameters

Following the SSM computations, larger iEDV was significantly associated with an aortic arch that had an oversized aortic root, followed by severely reduced ascending aorta that acutely transitioned into a wide transverse arch connecting to a smaller descending aorta. (r=0.414, p=0.019, Fig. 5) In this distinct shape pattern, the aorta was marked by the appearance of a pronounced 'indentation' or narrowing at the ascending aorta along with an exaggerated gothic-like transverse arch that is mismatched to the descending aorta. Supporting the association between higher iEDV with this aortic shape, significant positive correlations between iEDV and the traditionally measured iA_{surf}, iV, iA_{ventr}, and iT were discovered. (Table 1)

A similar aortic shape pattern, with a slightly reduced gothic appearance, was found to be significantly associated with increased SCP (r=0.412, p=0.024, Fig. 6).

1   In contrast, no associations between EF and 3D shape features were found via PLS analysis

2   of the deformation matrix (r=0.311, p=0.073), and no further correlations were found

3   between EF and traditionally measured morphometric parameters.

4   Both longer LICU and LOHS were associated with an aorta shape that had marked size

5   mismatch between the dilated transverse and the descending aorta (τ=0.290, p=0.025 and

6   τ=0.332, p=0.009, Fig. 7 and 8, respectively). In the case of the aortic shape associated with

7   longer LICU, there was an additional indentation in the ascending aorta. Using morphometric

8   measurements, high LICU was significantly associated with lower iA_{surf} (Table 1), while

9   LOHS was negatively associated with iCL (τ=-0.302, p=0.010, Table 1).

Discussion

Surgeons are trained to revise a reconstruction or anastomosis that does not have the correct or acceptable appearance. The concept of 'if it does not look right, it will not work right', regardless of actual hemodynamic significant consequences, is innate to most, if not all, cardiovascular surgeons. An unsatisfactory appearing reconstruction or anastomosis typically leads to unacceptable hemodynamic or flow characteristics that would require revision. However, the question remains if, in absence of important hemodynamic detriment, abnormal shape alone may still be associated with worse performance and outcomes. There is evidence indicating that in certain conditions, such as persistent systemic hypertension and left ventricular hypertrophy in presence of a gothic aortic arch following successful coarctation repair, morphology may be important. In patients with HLHS, the aortic root-ascending aorta-arch-descending aorta complex is obligatorily altered by the Norwood-type reconstruction, and the presence of hemodynamically significant obstruction is aggressively relieved either surgically or interventionally typically before TCPC completion, leaving though an abnormal arch shape. Therefore, HLHS patients represent a singular cohort where a quantitative assessment of the relationship between aortic shape and outcome is worthwhile.

In this study, using a novel 3D statistical shape analysis method (SSM), unique aortic arch features following Norwood-type HLHS palliation were found to correlate with increased iEDV, higher SCP prior to, and prolonged ICU and hospital stay after TCPC completion. This methodology, which combines CMR-based computational modeling and advanced statistical analysis, is based on defining a mean aortic arch that is representative of the average shape from a specific patient cohort. Adopting a template aorta based on subjects with normal hearts and normal aortic arch would be meaningless for HLHS patients due to the compulsory aortic arch reconstruction. Therefore, the template aorta (Fig. 4) is derived

from the 37 patient cohort as the 'norm' for a HLHS patient, with an enlarged aortic root as a consequence of the modified Damus-Kay-Stansel and the irregular aortic arch that is mismatched with a smaller descending aorta secondary to the patch augmentation. Free from obvious obstruction or acute changes in size and cross sectional area, this template would typically be one that surgeons and cardiologists would consider satisfactory.

From this template, the SSM quantified shape features or deformation vectors that correlated with increased iEDV and higher SCP prior to TCPC completion. It appeared that the common feature associated with these worse superior cavopulmonary circulation parameters is the marked loss of cross sectional area from the aortic root to the ascending aorta followed by an exaggerated and gothic-like transverse arch. The resultant distinct indentation or narrowing between the aortic root and the transverse arch has the appearance of an hour-glass. Interestingly, this feature was not associated with longer ICU or hospital stay following TCPC completion. Rather, it was pronounced mismatch between the transverse arch to the descending aorta and an overall smaller aortic arch that were correlated with these short-term outcome markers. It is particularly disheartening that 2 of the 3 subjects who have died among this cohort shared this particular shape feature. (Fig. 1c)

Despite uncovering these previously unknown relationships between aortic shape and clinical parameters, it is important to note that this study does not reveal any mechanistic insight as to why specific distortion or deformation in some shape features would be important, and thus cannot provide a causal relationship to our observations. Whether these deranged aortic shapes lead to altered impedance and/or perturbed aortic outflow, is unknown. Similarly, why iEDV and SCP, and not EF, prior to TCPC completion were affected cannot be answered. Nonetheless, in our previous study using wave intensity analysis in HLHS patients, impaired ventriculoarterial coupling was documented in patients whose aortic arch exhibited marked dilated and non-uniform transverse and descending arch morphology. (4) Therefore, this

study reconfirms that shape derangements alone can be associated with observable poorer outcomes in important clinical parameters. Further studies, perhaps with 4-D CMR and advanced computational fluid dynamics modeling, where realistic time-dependent and pulsatile flow/pressure characteristics can be simulated and examined, may yield important insights into the flow disturbances that can lead to worse cardiac function and clinical outcomes.

In conclusion, 3D statistical shape analysis revealed that independent of significant aortic arch obstruction, deranged arch morphology features in patients who underwent Norwood-type aortic arch reconstruction may be a potentially useful marker for outcome risks in HLHS patients. Aortic shape features that lead to hour-glass appearance between the aortic root and transverse arch, and exaggerated size mismatch between transverse arch and descending aorta, may be predictive of specific disadvantageous clinical outcomes.

Acknowledgements and Disclosures

References

1. Ou P, Bonnet D, Auriacombe L, Pedroni E, Balleux F, Sidi D, et al. Late systemic hypertension and aortic arch geometry after successful repair of coarctation of the aorta. Eur Heart J. 2004 Oct 1;25(20):1853–9.

2. Larrazabal LA, Tierney ESS, Brown DW, Gauvreau K, Vida VL, Bergersen L, et al. Ventricular Function Deteriorates With Recurrent Coarctation in Hypoplastic Left Heart Syndrome. The Annals of Thoracic Surgery. 2008 Sep;86(3):869–74.

3. Lee MGY, Brizard CP, Galati JC, Iyengar AJ, Rakhra SS, Konstantinov IE, et al. Outcomes of patients born with single-ventricle physiology and aortic arch obstruction: The 26-year Melbourne experience. The Journal of Thoracic and Cardiovascular Surgery. 2014 Jul;148(1):194–201.

4. Biglino G, Giardini A, Ntsinjana HN, Schievano S, Hsia T-Y, Taylor AM. Ventriculoarterial coupling in palliated hypoplastic left heart syndrome: Noninvasive assessment of the effects of surgical arch reconstruction and shunt type. The Journal of Thoracic and Cardiovascular Surgery. 2014 Oktober;148(4):1526–33.

5. Bruse JL, McLeod K, Biglino G, Ntsinjana HN, Capelli C, Hsia T-Y, et al. A Non-parametric Statistical Shape Model for Assessment of the Surgically Repaired Aortic Arch in Coarctation of the Aorta: How Normal is Abnormal? In: O Camara et al (Eds): Statistical Atlases and Computational Models of the Heart 2015. Munich: Springer International Publishing Switzerland 2016; 2016. p. 1–9.

6. Leonardi B, Taylor AM, Mansi T, Voigt I, Sermesant M, Pennec X, et al. Computational modelling of the right ventricle in repaired tetralogy of Fallot: can it provide insight into patient treatment? Eur Heart J Cardiovasc Imaging. 2013 Apr;14(4):381–6.

7. Durrleman S, Prastawa M, Charon N, Korenberg JR, Joshi S, Gerig G, et al. Morphometry of anatomical shape complexes with dense deformations and sparse parameters. NeuroImage. 2014 Nov 1;101:35–49.

8. Antiga L, Piccinelli M, Botti L, Ene-Iordache B, Remuzzi A, Steinman DA. An image-based modeling framework for patient-specific computational hemodynamics. Med Biol Eng Comput. 2008 Nov 1;46(11):1097–112.

9. Besl PJ, McKay ND. A method for registration of 3-D shapes. IEEE Transactions on Pattern Analysis and Machine Intelligence. 1992 Feb;14(2):239–56.

10. Piccinelli M, Veneziani A, Steinman DA, Remuzzi A, Antiga L. A framework for geometric analysis of vascular structures: application to cerebral aneurysms. IEEE Trans Med Imaging. 2009 Aug;28(8):1141–55.

11. Durrleman S, Pennec X, Trouvé A, Ayache N. A forward model to build unbiased atlases from curves and surfaces. In: Pennec, X, Joshi, S (eds) Proc of the International Workshop on the Mathematical Foundations of Computational Anatomy,. 2008.

12. Joliffe, I.T. Principal Component Analysis. 2nd ed. Springer-Verlag New York, Inc.; 2002.

13. Mansi T, Voigt I, Leonardi B, Pennec X, Durrleman S, Sermesant M, et al. A Statistical Model for Quantification and Prediction of Cardiac Remodelling: Application to Tetralogy of Fallot. IEEE Transactions on Medical Imaging. 2011;30(9):1605–16.

14. Daszykowski M, Kaczmarek K, Vander Heyden Y, Walczak B. Robust statistics in data analysis — A review: Basic concepts. Chemometrics and Intelligent Laboratory Systems. 2007 Feb 15;85(2):203–19.

1 **Table 1**

2 Correlations between traditionally measured 2D and 3D parameters and clinical parameters

3 of interest. Lower case *i* indicates parameters indexed to patient BSA.

Correlations	EF [%] N = 37	iEDV [ml/m²] N = 37	SCP [mmHg] N = 33	LICU [days] N = 37	LOHS [days] N = 37
iA_{surf} [mm²/m²]	r=-0.047 (p=.782)	**r=0.399* (p=.014)**	r=0.039 (p=.831)	**τ=-0.261* (p=.029)**	τ=-0.089 (p=.446)
iV [mm³/m²]	r=-0.051 (p=.765)	**r=0.357* (p=.030)**	r=-0.051 (p=.776)	τ=-0.195 (p=.102)	τ=-0.003 (p=.979)
A_{surf}/V [1/mm]	r=-0.027 (p=.875)	r=-0.276 (p=.098)	r=0.083 (p=.645)	τ=0.088 (p=.460)	τ=-0.176 (p=.134)
iA_{ventr} [mm²/m²]	τ=-0.005 (p=.969)	**τ=0.291* (p=.011)**	τ=-0.094 (p=.461)	τ=-0.107 (p=.370)	τ=0.025 (p=.834)
$iA_{nativeAo}$ [mm²/m²]	τ=0.008 (p=.948)	τ=0.027 (p=.814)	τ=-0.214 (p=.093)	τ=-0.126 (p=.291)	τ=-0.028 (p=.813)
iA_{trans} [mm²/m²]	r=-0.247 (p=.141)	r=0.164 (p=.332)	r=-0.094 (p=.603)	τ=0.025 (p=.833)	τ=0.126 (p=.281)
iA_{isth} [mm²/m²]	τ=0.071 (p=.539)	τ=0.099 (p=.388)	τ=0.050 (p=.695)	τ=-0.151 (p=.205)	τ=-0.006 (p=.958)
iA_{dia} [mm²/m²]	τ=0.179 (p=.120)	τ=0.207 (p=.071)	τ=0.102 (p=.424)	τ=-0.116 (p=.329)	τ=-0.006 (p=.958)
$A_{nativeAo}/A_{ventr}$	τ=0.005 (p=.969)	τ=-0.048 (p=.676)	τ=-0.170 (p=.183)	τ=-0.066 (p=.580)	τ=0.000 (p=.999)
A_{trans}/A_{ventr}	r=-0.274 (p=.101)	r=0.024 (p=.886)	r=-0.075 (p=.676)	τ=0.069 (p=.562)	τ=0.108 (p=.358)
A_{isth}/A_{trans}	τ=0.077 (p=.505)	τ=-0.054 (p=.638)	τ=0.086 (p=.500)	τ=0.013 (p=.916)	τ=-0.090 (p=.446)
A_{isth}/A_{dia}	τ=-0.074 (p=.522)	τ=-0.012 (p=.917)	τ=-0.062 (p=.627)	τ=-0.072 (p=.544)	τ=-0.003 (p=.979)
A_{dia}/A_{trans}	τ=0.200 (p=.082)	τ=-0.021 (p=.855)	τ=0.072 (p=.572)	τ=-0.132 (p=.268)	τ=-0.059 (p=.618)
iCL_{length} [mm/m²]	r=-0.149 (p=.379)	r=0.277 (p=.097)	r=0.049 (p=.785)	τ=-0.179 (p=.133)	**τ=-0.302* (p=.010)**
CL_{tort}	r=-0.037 (p=.826)	r=-0.131 (p=.440)	r=0.044 (p=.806)	τ=-0.223 (p=.061)	τ=-0.099 (p=.401)
iT [mm/m²]	r=0.079 (p=.642)	**r=0.562** (p<.001)**	r=-0.056 (p=.756)	τ=-0.044 (p=.712)	τ=-0.096 (p=.415)
iD_{asc} [mm/m²]	r=0.254 (p=.129)	r=0.263 (p=.115)	r=-0.018 (p=.919)	τ=-0.053 (p=.654)	τ=-0.160 (p=.172)
iD_{desc} [mm/m²]	τ=0.095 (p=.410)	τ=0.012 (p=.917)	τ=0.110 (p=.389)	τ=-0.088 (p=.460)	τ=-0.111 (p=.344)
D_{desc}/D_{asc}	τ =-0.080 (p=.488)	τ=-0.084 (p=.464)	τ=0.150 (p=.240)	τ=-0.060 (p=.616)	τ=-0.062 (p=.599)

4

1

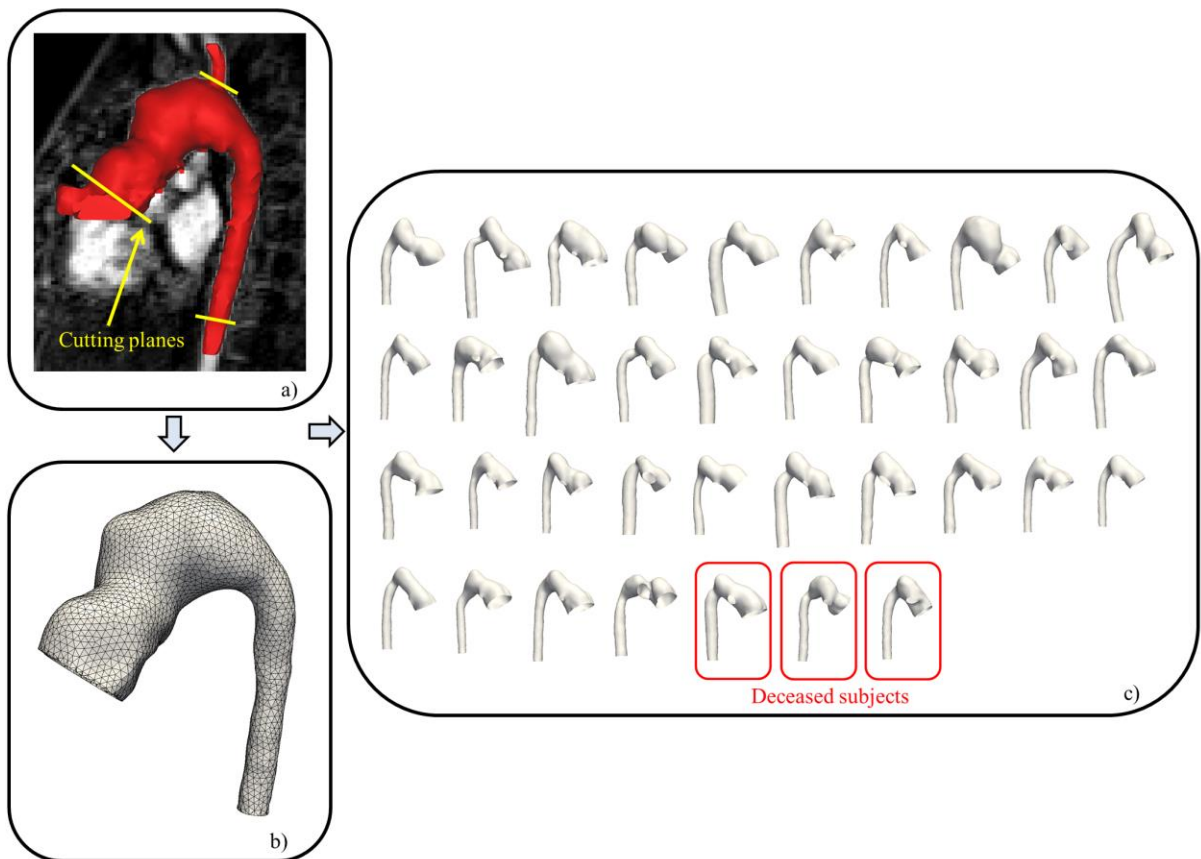2   **Table 2**

3   Traditional geometric parameters were measured on each arch model and averaged to obtain

4   the respective population mean. The same parameters were then measured on the computed

5   template aorta and compared to its population mean. Low deviations confirmed the template

6   aorta to be a good estimate of the 3D mean shape of our population.

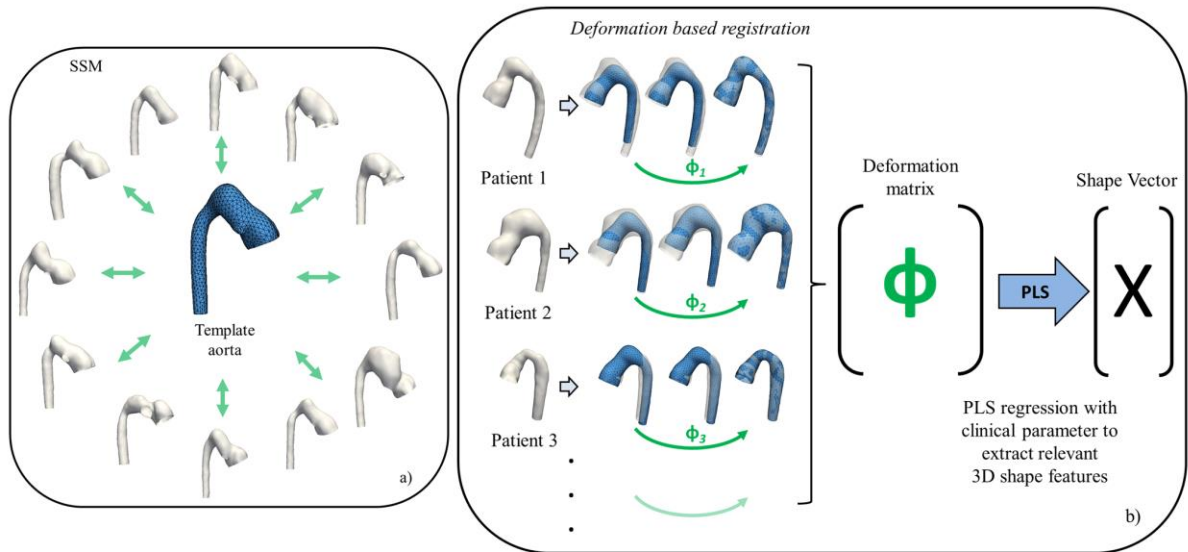| *Deviations*	**Population mean**	**Measured on template shape**	**Template deviation from population mean [%]**
A_{surf} [mm²]	5519.35	5629.81	+2.00
V [mm³]	21628.63	22000.62	+1.72
A_{surf}/V [1/mm]	0.2635	0.2559	-2.90
CL_{length} [mm]	107.12	104.75	-2.21
CL_{tort}	0.726	0.711	-2.05
Overall absolute	-	-	***2.17***

7

1
Figure Legends

2

3 **Fig. 1:** Aortic arch volumes were segmented from CMR data and cut at the sub-annular plane

4 and at the level of the diaphragm; head and neck, and coronary vessels as well as the native

5 aorta were cut off as close as possible to the arch; cutting planes marked (a). 3D surface

6 meshes (b) of all 37 patients constituted the input for the statistical shape model (c). 3
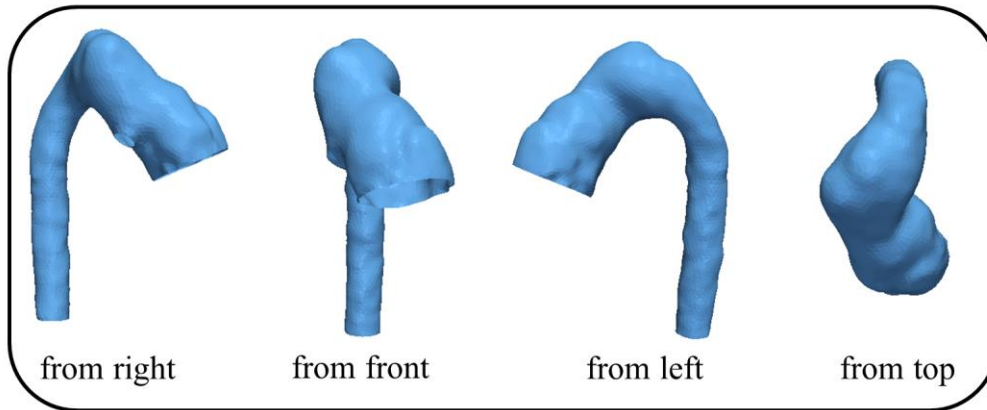
7 patients who deceased are marked in red.

1

2 **Fig. 2:** Traditional 3D (surface area A_{surf}, volume V, centerline length CL_{length} and tortuosity

3 CL_{tort}) and 2D measurements (arch width T, ascending D_{asc} and descending D_{desc} aortic

4 diameters) were taken on the 3D surface models (a) and on the 2D CMR image data of each

5 patient (b). Width T, D_{asc} and D_{desc} were measured at the mid-level of cavopulmonary
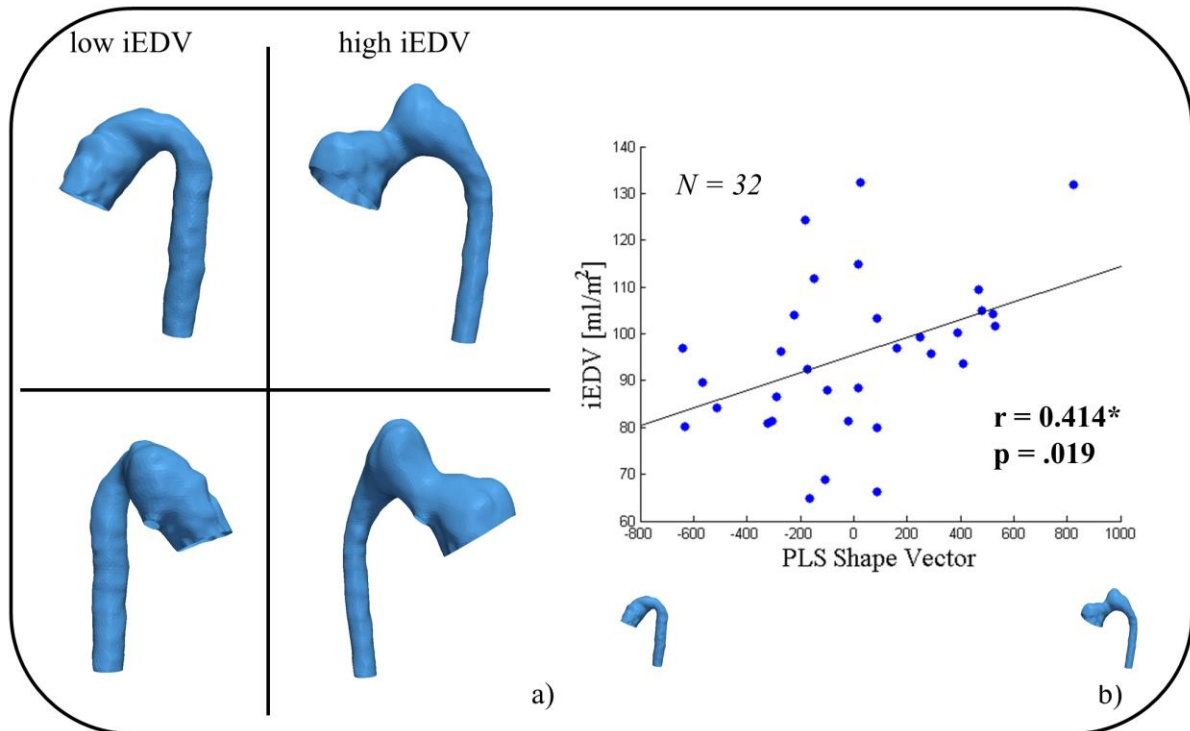
6 (Glenn) connection as marked.

1

Fig. 3: The SSM computes the 3D mean anatomic aorta shape, called *template* from a population of arch shapes provided as surface meshes (a). Instead of its point coordinates, each patient shape is uniquely defined by its specific set of deformation vectors Φ_i, registering the template aorta to each patient shape (b). All deformations Φ taken together build the deformation matrix, containing all 3D shape information of the population. The 3D shape features most related to a clinical parameter are extracted from the deformation matrix via partial least squares regression analysis (PLS). Results can be visualized as 3D deformation of the template aorta and quantified via the numerical *shape vector* X, describing how much of the extracted shape features is contained within each patient arch shape.

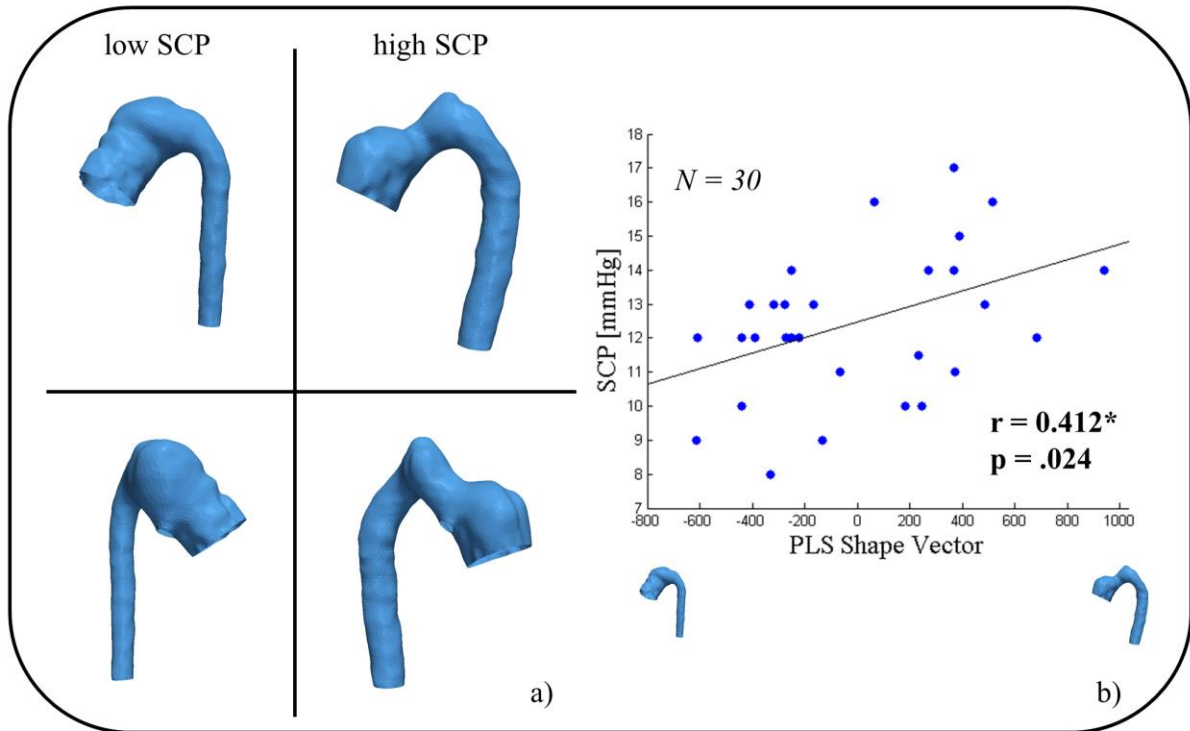from right   from front   from left   from top

Fig. 4: The computed template aorta (i.e. 3D mean shape of the population) showed a mildly

dilated aortic root and transverse arch, no significant coarctation and a slightly tortuous arch.

The template can be seen as a "prototype" of our HLHS arch population.
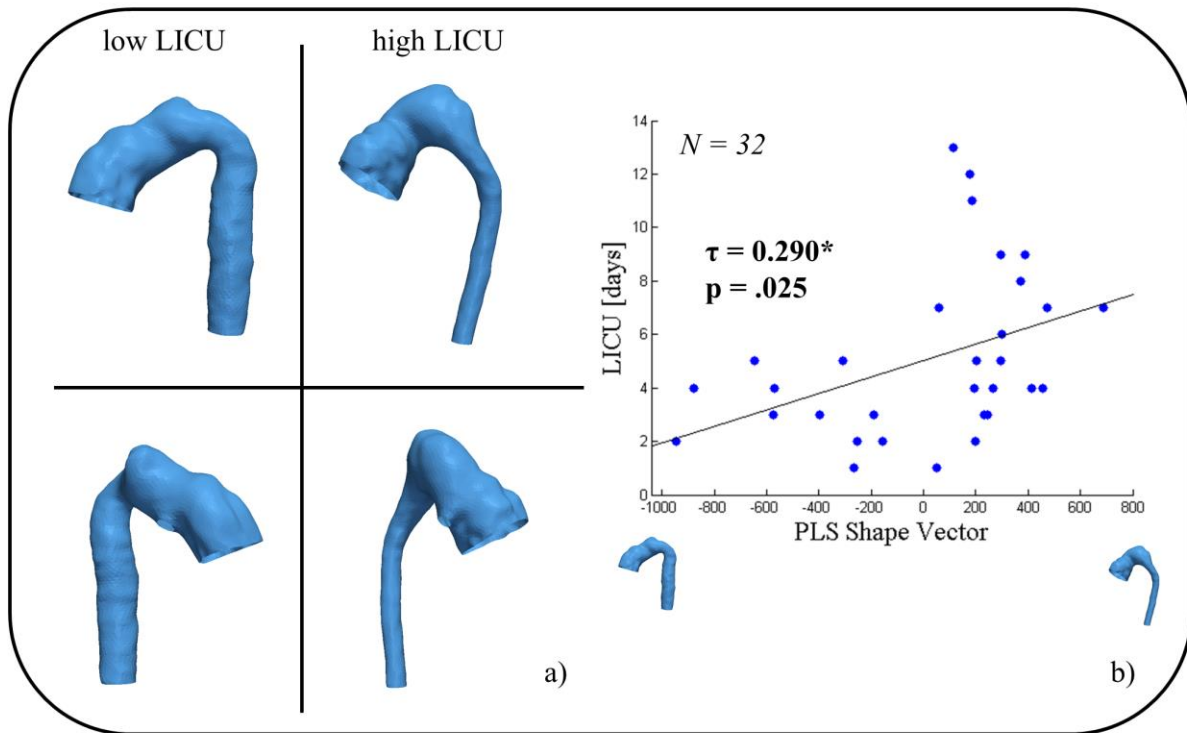
1

2 **Fig. 5:** 3D shape features most related to differences in iEDV are visualized as deformations

3 of the template aorta (a; from left side, top; from right side, bottom). High iEDV was mainly

4 associated with an overall large and wide arch with a size mismatch and distinct indentation

5 in the ascending aorta. Results were confirmed by traditional correlation analysis between

6 iEDV and the extracted PLS shape vector (b): patients with high shape vector values, thus

7 having (among others) arch shape features as visualized for high iEDV presented with high

8 iEDV as measured from CMR. 5 patients were found to be outliers in terms of BSA and/or

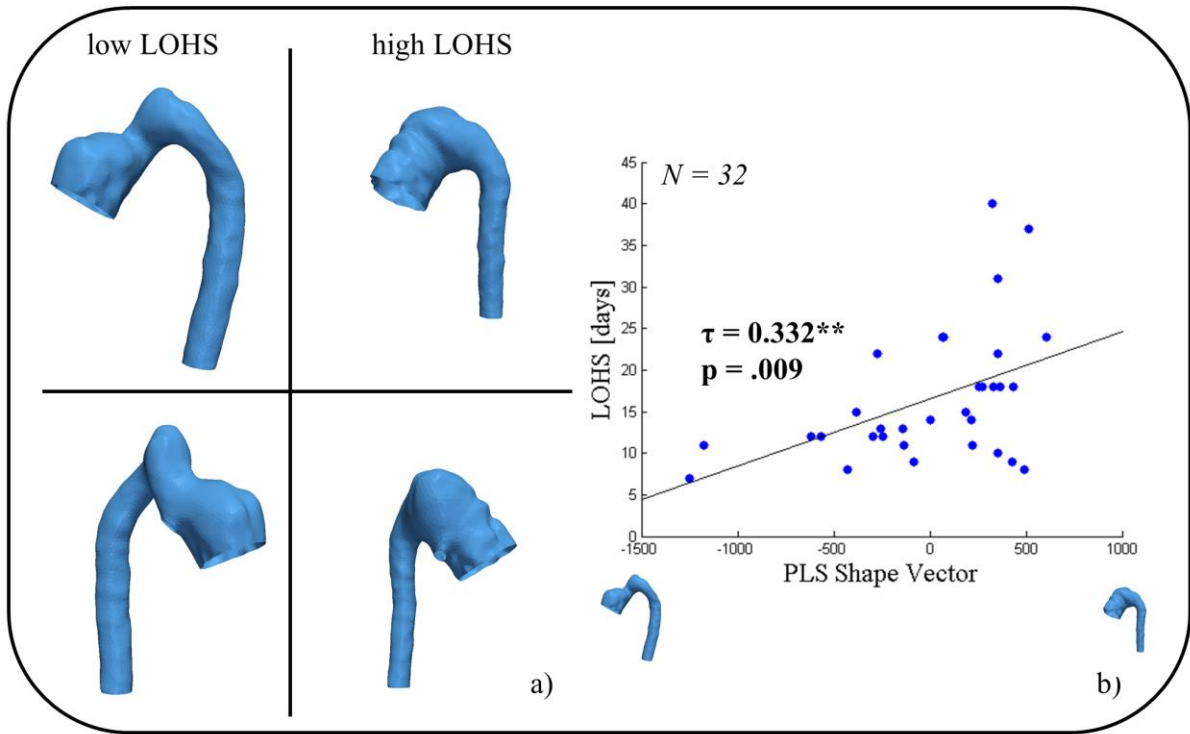9 iEDV and were thus excluded from the regression analyses.

Fig. 6: High SCP was associated with a wide, slightly gothic arch shape, a dilated root and a distinct indentation in the distal ascending arch (a). However, the arch continuation post indentation showed to be rather uniform in size. 4 patients did not have SCP recorded and 3 patients were found to be outliers and were thus excluded from the regression analyses.

Fig. 7: Long stay in ICU (LICU) after TCPC completion correlated significantly with an overall smaller, shorter but wide arch, showing a slight indentation in the ascending aorta and a severe size mismatch between dilated transverse and slim descending aorta (5 regression outliers excluded).

1

2 **Fig. 8:** Long hospital stay (LOHS) after TCPC completion was associated with an overall

3 smaller and short arch with a dilated root and transverse arch, resulting in distinctly non-

4 uniform arch continuation towards the descending aorta and size mismatch (5 regression

5 outliers excluded).